HHS Public Access

Author manuscript

J Org Chem. Author manuscript; available in PMC 2021 August 07.

Published in final edited form as:

J Org Chem. 2020 August 07; 85(15): 9447–9453. doi:10.1021/acs.joc.0c00349.

Next-Generation TLC: A Quantitative Platform for Parallel Spotting and Imaging

Alexander A. Boulgakov[1,†], **Sarah Moor**[2,†], **Hyun Hwa Jo**[2,†], **Pedro Metola**[2], **Leo A. Joyce**[3,4], **Edward M. Marcotte**[1], **Christopher J. Welch**[*,3,5], **Eric V. Anslyn**[1,*]

[1]Center for Systems and Synthetic Biology/Institute for Cellular and Molecular Biology, Department of Molecular Biosciences, The University of Texas at Austin, Austin, Texas 78712, United States

[2]Department of Chemistry, The University of Texas at Austin, Austin, Texas 78712, United States

[3]Department of Process Research and Development, Merck & Co., Inc., Rahway, New Jersey 07065, United States

[4]Current address: Arrowhead Pharmaceuticals, Inc, 502 S. Rosa Rd., Madison, WI 53719, United States

[5]Current Address: Indiana Consortium for Analytical Science and Engineering, Indianapolis, Indiana, 46202, United States

Abstract

A high-throughput screening (HTS) approach for simultaneous analysis and quantification of the percent conversion of up to 48 reactions has been developed using a thin-layer chromatography (TLC) imaging method. As a test-bed reaction, we monitored 48 thiol conjugate additions to a Meldrum's acid derivative (**1**) in parallel using TLC. The TLC elutions were imaged using a cell phone and a LEGO™ brick-constructed UV/vis light box. Further, a spotting device was constructed from LEGO™ bricks that allows simple transfer of the samples from a well-plate to the TLC plate. Using software that was developed to detect "blobs" and report their intensity, we were able to quantitatively determine the extent of completion of the 48 reactions with one analysis.

Introduction

Drug discovery and synthesis optimization rely on modern catalysis to continue advancing. Finding cost-effective routes to both new and existing drugs is a constant area of investigation.[1] High-throughput experimentation (HTE) allows hundreds to thousands of different reaction permutations to be run in a matter of hours and is widely used in the

*Corresponding Authors: anslyn@austin.utexas.edu. christopher@welchinnovation.com.
†These authors contributed equally.

Supporting Information

The Supporting Information is available free of charge on the ACS Publications website.

General procedure, synthesis and characterization of EVA, TLC Analysis, ^{1}H NMR and LC/MS spectral data for reaction 1 yield analysis, Appaloosa Thin Layer Chromatography Wizard User Manual (PDF)

pharmaceutical industry for discovering ligands for receptors, kinases, and enzymes, along with optimizing reaction conditions.[2] For HTE to succeed, a complimentary high-throughput screening (HTS) protocol must be created, otherwise simply by virtue of the multitude of samples, the analysis becomes the bottleneck in the overall discovery process.[3] Although many researchers have developed rapid assays for yield determination, the need for more cost-effective assays that do not require specialized or expensive equipment remains.[1] Combining existing separation assays, in this case TLC, with now ubiquitous smartphone capabilities shows promise in addressing these needs.

Thin layer chromatography (TLC) is one of the most common chromatography techniques used by synthetic chemists to identify compounds in a mixture, determine their purity, and follow the progress of a reaction.[4] Visualization usually occurs under UV light or by using staining reagents. In the last couple of decades, a number of innovative improvements in TLC have emerged.[5–7] These have included quantitative analysis via optical scanning, such as is done with commercial TLC scanners.[8] There have been examples of photometric procedures followed by image processing, as well as using mass spectrometry on the eluted spots.[9,10] However, these techniques have been used to test the purity of the samples rather than monitoring reaction progress and/or determining reaction yield.[11] Furthermore, none of the approaches allow for the analysis of multiple reactions simultaneously.

Our group had previously reported a single example of TLC imaging, in this case to pre-screen various conditions of a Ircatalyzed allylation reaction to quantitatively determine their yields.[12] As both the starting material and the product were UV active, we were able to correlate their concentrations to their corresponding spot intensities as observed under UV irradiation. In this report, we extensively expand on this methodology and describe a HTS platform created by combining a TLC multi-spotter, a light box built from LEGO™ bricks and spotting device (*vida infra*), an alternating offset arrangement of TLC spots designed to allow for 48 simultaneous analyses, as well as advances in spot-recognition imaging software.

The choice of reaction chemistry to demonstrate the methodology was immaterial to our goals, except that we sought a reaction where conditions could be easily varied. Additionally, although spot-staining for visualization can readily be used in our approach, we sought a reaction where the starting materials and products were UV active. With these considerations in mind, we chose the reaction of a Meldrum's acid derived conjugate acceptor **1** with various nucleophiles that act as exchangeable units (E.U.s, Scheme 1).[13] Compound **1** allows for a coupling of amines and thiols, which can then be decoupled to their starting components using dithiothreitol (DTT). Although this method could provide even more useful for "cleaner" reactions (i.e. a reaction that gives only one product) to get the yield of the reaction rather than conversion, we chose this exchange reaction to demonstrate the full scope of this technique.

Although **1** has been successfully used for various biological and materials applications, little work has been put into optimizing the thiol or amine exchange reactions. The thiol scrambling is tricky to quantify because it often requires sparging to remove methyl mercaptan. While conventional HPLC analysis is a promising method to monitor this

reaction, the sequential elution of each individual sample can make this a tedious, time-consuming method to use for larger scale parallel optimization experiments.[1] TLC, on the other hand, enjoys the relative advantages of low cost, the ability to analyze impure samples, the availability of analyte-specific visualization reagents, and the ability to carry out multiple simultaneous analyses by spotting multiple samples on each plate and developing several plates in parallel.[14] This parallel analysis capability, along with the fact that TLC imaging has been previously reported,[8–10] led us to make several improvements such that TLC would be more amenable to HTS. In this paper, we report a method to analyze parallel synthesis procedures in 96-well plates, albeit any plate format is amenable to what is now described.

Results and Discussion

Our goal was to spot 12 reactions at a time from a 96-well plate (8 × 12 strips) wherein the reactions of Scheme 1 were performed using amines and thiols as the exchangeable units (E.U.s, Supplementary Table 1). Although 96-reactions could have been screened, the methodology now described was most successful with only half the plate, i.e. 48 reactions. The amount of sample delivered and the spreading during spotting can affect both resolution and smearing of the eluted spots. Thus, as any practitioner of TLC knows, the spotting of the plate is crucial to success. As many of the reactions of compound **1** with amines or thiols give multiple products (mono-substituted, di-substituted, and polymerized), failing to properly control amounts dispensed would result in eluted product spots that are too broad and hence show extensive overlap with spots from other lanes. For this reason, it was vital to have a TLC spotter that would dispense small initial volumes (< 1 μL), yet sturdy enough to place all 12 spotters flat on the plate.[15,16] While we initially created a hand held 3D-printed spotter that accommodated 12 steel needles, the operator needed to carefully touch all 12 needles at once to the silica on the plate and press lightly so that the needles are not plugged with silica. The fact that the spot intensity across the 12 needles was dependent upon careful control by the operator prompted us to devise a less variable spotting method.

We turned to the use of a LEGO™ spotter, shown in Figure 1, as a design for those labs that do not have access to a 3D-printer, and/or operators with slightly shaky hands. This easy to assemble, user-friendly setup, yields the capability to perform spotting in a reproducible, staggered manner (to obtain 4 rows of 12 spots, i.e. 48 spots in total) and the added potential for customization. The first part of the spotter is a holder where the 12 blunt-nosed needles are arranged linearly in regular intervals using a mounting-piece created from a pipette tip box (Figure 1a). The second piece is the base of the spotter (carriage), which consists of a cavity to hold the TLC plate on two sliding panels with two sets of three removable spacers (Figure 1b). Once the carriage is loaded with the holder, the four columns on the sides allow for vertical movement perpendicular to the plane of the TLC plate that provides the spotting (Figure 1c). The holder can be detached from the carriage for loading of the samples from an installed 96-well plate, and then reassembled to allow for spotting of an installed TLC plate. This later operation must be conducted using both hands and adjusting the timing of contact between tips and plate to ensure uniform and efficient spotting. Importantly, due to the controlled sliding of the holder up and down along the 4 posts, the needles all touch simultaneously and therefore reduces operator error. Once the first row of 12 samples are spotted, the 2 sets of spacers come into action: removing one spacer in each set allows two

sliders to move (one along the X axis and the other along the Y axis) before performing the next round of 12 sample spotting, which thereby occurs slightly to the right and above the initial row of 12 spots. The movement of the sliders is akin to playing hop-scotch, where one jumps to the right and then forward, thus moving diagonally a controlled distance. This operation is repeated three times for the total of 48 samples before the TLC is developed and analyzed in a LEGO™ black box (Figure 1d). After each spotting of the TLC plate, the needles are emptied by touching filter paper and a wash with acetone to remove excess solution so as to not contaminate the next set of 12 spots.

In a previous report we described the use of a LEGO™ black-box as a simple and inexpensive alternative to a fluorescence 96-well plate reader.[14] Herein, a variant was used for visualization of the TLC plates with a common UV lamp, with data recording via cell phone photography, followed by the use of chromaticity/luminosity for data analysis (*vida infra*). The LEGO™ loading stage was modified to hold TLC plates (Figure 1d) rather than 96-well plates. This simple modification demonstrates one strength of using LEGO™ bricks for the construction of instruments rather than 3D-printing. The device can be easily reconfigured for numerous purposes without the generation of a new CAD-file and the time taken for printing. This is further exemplified with the above described TLC spotter. Albeit some time was taken to imagine the operations and then optimize the apparatus, creating such a device with moving parts out of materials other than LEGO™ bricks would have been significantly more challenging and more expensive to repair or replace when needed.

For analysis of reactions in a standard 96-well plate, we explored the direct spotting of rows of samples (0.9 mm well to well spacing) onto a standard 20 × 20 cm TLC plate. Only a single complete row of 12 spots can fit onto a single TLC plate, and while strategies for interleaving additional rows of spots along the origin line are possible, we found the resulting developed TLC plates to be highly congested and difficult to interpret. Thus, we investigated an alternative spotting strategy in which spots from rows A, B, C, D, *etc*. are offset in both the horizontal and vertical direction (Figure 2). Interestingly, modeling using 96-spots shows this technique to produce a profile of product spots that takes the form of a skewed 8 × 12 grid when the R f of the eluted compound of interest are all the same and between about 0.3 and 0.6 (Figure 2a), with higher or lower R_f values producing congested images that are difficult to interpret. Demonstration of the approach is shown in Figure 2b, where a 96-well microplate containing a mixture of two dyes: methylene blue ($R_f \sim 0$) and methyl red ($R_f \sim 0.6$) is eluted using 95% ethanol/water. The red dye elutes up the plate while the blue dye stays at the baseline. The analysis of a TLC plate containing 4 wells with higher levels of methyl red affords, not eluted, gives a straightforward identification of the ‘address’ of these spots (Figure 2c).

Having demonstrated that 12 reactions can be spotted in a row, and the next 12, and so forth, in a diagonally staggered manner to minimize the interference from the spots when the plate is developed, we turned our attention to photographic plate imaging. To start, a computer-generated image of identical non-eluted spots was created to demonstrate the accuracy of the software (Figure 3a).

Forty-eight spots were used to emulate reaction spots. These spots were then analyzed by the software with an average deviation of 1.6 (Figure 3b). However, as these spots were computer generated and TLCs are subject to human error, we expected that real plates analysis would not be so accurate. However, these promising results prompted us to analyze complex reaction mixtures.

In our preliminary report of TLC quantitative imaging for determining reaction yield, we generated a calibration curve for the spot intensity of the product.[12] In the current study, we created a calibration curve to demonstrate how concentration can be detected and quantified using our image analysis program (*vida infra*). Nine samples of varying concentrations of **1**, ranging from 20 to 200 μM, were spotted on a plate and eluted with 3:1 hexanes/ethyl acetate (*v:v*). Figure 4a shows a photo taken with an iPhone using the black-box constructed of LEGO™ bricks under UV radiation (Figure 1).[14] The solvent system was devised such that the spots have an R_f value of 0.5 (*vida supra*), and all spots on the plate were automatically detected and the intensity of each spot was measured using an algorithm that we developed (Figure 4b, details below). By plotting the measured intensity versus concentrations of **1**, a calibration curve was generated (Figure 4c). Here, 200 μM of **1** corresponds to 100% of **1** remaining in a reaction of any well in the plate, while lower spot intensities are used to estimate the % completion of the reaction. This demonstrates the software's ability to quantify different spot concentrations.

The conjugate addition reaction with **1** was performed in methanol with various amines and thiols (Supplementary Table S1) in 48 wells of a 96-well plate for 36 h (initial conc. of **1** = 0.25 mM). We used 48 reactions rather than 96 because the overlap of the spots was too severe when 96 samples of varying R_f values for the products were spotted. All the reactions were performed in a 96 deep-well plate and were then spotted on to the silica plate using the in-house LEGO™ spotter and the experimental details given above associated with our discussion of Figure 1a. Using the spotting configuration discussed above, the 48 reactions were eluted in 3:1 hexanes/ethyl acetate (*v:v*). The eluted spots were then analyzed using our processing script to get starting intensities for each well, as now described.

TLC plate images were analyzed in a semi-automated fashion to measure spot intensities for each analyte. These intensities were then used to determine the reaction yields based on the average control starting **1** spot intensity as described below (Supplementary Table S1). But first, we describe the image processing steps used. While the ultimate plan is for an interactive smart-phone app to semi-automatically analyze the TLC plates with assistance from the user, for now we have developed a desktop GUI that accomplishes this task. Our code is available on Github at https://github.com/marcottelab/appaloosa, with a sample image and a walkthrough manual to get started. It primarily utilizes Scikit-Image for its image morphology routines[15]. We begin the analysis of each image by cropping it to the plate and converting it to grayscale, so that spots are dark objects on a light background. This grayscale image is then median corrected to standardize brightness across the plate and remove any bias due to positioning of the UV/vis lamp on the LEGO™ box. To identify reaction spots, we perform one round of waterfall segmentation to isolate areas containing spots from the background, and then to this isolated foreground we apply one round of watershed segmentation to subdivide it into spots corresponding to individual reactions.[17,18]

Both waterfall and watershed segmentations treat pixel values in an image as a terrain, as in a grassy knoll. In this analogy, each dark spot forms a depression—or drainage ditch—that are isolated from their neighbors along ridge lines analogous to dividing ranges in geography, or boundaries of counties/cities on a map. The waterfall algorithm is more wary of over-segmentation and is hence applied before the more sensitive watershed algorithm. If we were to apply a watershed segmentation immediately, without the initial waterfall round, we would be likely to "identify" many spurious "spots" in the background. Hence the need for a two-round approach

Although we have chosen the default parameters used by the second segmentation step to work well with the majority of TLC plates, sometimes the resulting segmentation is not sufficiently fine-grained enough to separate spots that are very faint or blur together. In such cases, we rely on the user to direct the software via the interactive GUI. The user can direct the software to attempt a finer-grained sub-division of a particular spot, or to manually subdivide spots by hand. We provide examples of each operation in our Github walkthrough. Note that such manual subdivisions can be applied iteratively until a satisfactory result is obtained, making the interactive aspect of our software very powerful. Finally, it is possible to cast all identified spots into circles. This is accomplished by identifying potential circular features of each spot with a Laplacian of Gaussian[19], and then from these choosing the circular feature (*i.e.* circle) that maximizes the average intensity per unit area as captured by the circle. Figure 5 shows an example eluted TLC plate with a final spot segmentation, including both automatically-and manually-segmented spots, all finally converted into circles around the spot. Another useful functionality in the GUI is the ability of the user to manually define the baselines for reactions, as well as the solvent front. Once this is done, it is possible to assign spots to different baselines and from this their R_f values can be calculated. Again, our walkthrough provides an example.

Once the spots are segmented, we measure their intensity against the background as a proxy for analyte amount. We take the sum of pixel values within a segmented spot as its raw intensity. To obtain background intensity, we scale the spot's bounding box to twice its area, and then take the median of pixel intensities within the box that are outside of any other adjacent segmented spots. We correct for the background by subtracting from the raw intensity the background intensity multiplied by the area of the spot (across which pixels were summed).

Once all the software had been developed, we turned to actual TLC analysis using **1** and various E.U.s (Supplementary Table S1). We assigned a subset of the wells as control reactions (#5, #18, #31 and #44, Supplementary Table S1) to have no E.U.s. These wells were chosen to give a distribution of spots across the plate to account for differences in lamp light. Thus, the resulting spots would be solely due to **1** which has a $R_f = 0.38$. Using the GUI interference, we can manually extrapolate the solvent front position to calculate R_f values. By marking the starting position of each baseline, we can assign eluted spots to the original baseline positions (i.e. one of four), as well as classify whether they are unreacted analyte (*i.e.* whether they lie on a corresponding $R_f = 0.38$ lines). To calculate the extent of reaction and compare to the average intensity of the control reactions, and calculate the amount of reacted *vs.* unreacted starting material (Supplementary Table S2). This is done for

all 48 spots. From the measured spot intensities, the concentration of **1** remaining in the reaction was calculated using the starting intensity of the **1** control samples, well #5, #18, #31 and #44, which had an average intensity of 71. The concentration data can then be converted to percent of **1** remaining after 36 h, which allows us to estimate conversion of the reaction. Of course, as done in our previous report, the calibration curve Figure 3 can alternatively be used to quantitate remaining starting material.[12]

In order to test the accuracy of the data collected, LC/MS was performed on ten randomly selected reactions to estimate percent starting material remaining. When the two values were compared, the average absolute difference between starting material as detected by LC/MS and TLC was 9%. Although the average error is quite low, the error associated with some reactions was significantly higher than this average. Looking closer, the reactions can be classified into two rather distinct groups: the first, with 7 out of 10 reactions, which did not suffer spot overlap and hence were accurately quantified with an average absolute error 3%; and the second, with the remaining 3 out of 10 reactions, which suffered spot overlap and hence were quantified with an average error of 25% (which is still rather informative in many cases). The larger errors in the second group can be attributed to overlap between the adjacent spots, in some cases when they were initially spotted and others after the plate was run. For example, 1,4-butanedithiol (spot 4, Supplementary Figure S1), has significant overlap with its adjacent spot. Such errors can be remedied with careful spotting or if cleaner reactions were screened. In addition, due to the unique shape of our TLC plate, an improvised TLC chamber was used which results in some slight curving of the TLC spots as the plate was eluted. Thus, the TLC method gave an error of under 10% in determining extent of reaction of **1** with the various E.U.s.

Having found success with a parallel analysis of 48 reactions via TLC for HTS purposes, it is important to discuss limitations and complications. First, we are relying on a UV-lamp, and the kind of lamp, how long one waits to take the picture after turning on the lamp, all effect the images. Second, the camera you use, or the box (i.e. the darkness of the surroundings) will influence the result as well. Any overlap between spots will affect adjacent spots making it imperative to have the spots properly staggered and ensuring the TLC runs straight. Lastly, consistency in spot size and between the analysis and calibration plates is critical, and the LEGO™ spotter nicely assists in this regard. However, as long as one is consistent with all the experimental procedures and settings, our overall TLC methodology gives reliable data that can be used to quantitate the yield and/or % completion of numerous reactions simultaneously. While this manuscript focused on optical detection of TLC spots, an analogous approach may prove useful for DESI or MALDI mass spectroscopy imaging of TLC plates.

Summary

TLC is the most common bench-side quick analytical test for examining the progress of chemical reactions. While multiple TLC spots along a single line is common for qualitatively analyzing various samples collected from flash-chromatography, such spotting has not been previously converted to a parallel method for reaction screening and yield quantitation. The overall approach described herein for analyzing ½ of a 96-well plate is

simple, fast, and user friendly. It involves a 12-needle dispensing device constructed from LEGO™ bricks, a LEGO™ black-box for photography, and an extensive software suite available on Github. We anticipate that his work will facilitate reaction discovery and optimization, as well as inspire further improvements on this classic and simple analytical method.

Experimental

Conversion Validation:

Stock solutions (40 mM, 0.02 mmoles) of each compound (Supplementary Table S1) and EVA (40 mM, 0.02 mmoles) were made in MeOD. From the stock solutions of each compound and EVA, 500 μL of each were mixed in a 1:1 ratio in vials and left to sit for 48 hours. After 48 hours, 1 mL of a 20 mM stock solution of 1,3,5-trimethoxybenzene was added in a 1:1 mixture with the reaction mixtures. The samples were then analyzed via NMR. For N-benzylmethylamine, the reactions mixture along with the control reaction were diluted with MeOD and analyzed via LC/MS.

Supplementary Material

Refer to Web version on PubMed Central for supplementary material.

ACKNOWLEDGEMENTS

We gratefully acknowledge support from the following funding sources: National Science Foundation to A.A.B. (DGE-1610403), and an NSF GOALI (1665040), the National Institute of Health (1 S10 OD021508-01), the Howard Hughes Medical Institute (GT10481), and the Welch Regents Chair to EVA (F-0046). EMM acknowledges funding from the NSF, NIH, and Welch Foundation (F-1515).

REFERENCES

(1). Herrera BT; Pilicer SL; Anslyn EV; Joyce LA; Wolf C Optical Analysis of Reaction Yield and Enantiomeric Excess: A New Paradigm Ready for Prime Time. J. Am. Chem. Soc 2018, 140 (33), 10385–10401. 10.1021/jacs.8b06607. [PubMed: 30059621]

(2). Krska SW; DiRocco DA; Dreher SD; Shevlin M The Evolution of Chemical High-Throughput Experimentation To Address Challenging Problems in Pharmaceutical Synthesis. Acc. Chem. Res 2017, 50 (12), 2976–2985. 10.1021/acs.accounts.7b00428. [PubMed: 29172435]

(3). Mayr LM; Fuerst P The Future of High-Throughput Screening: J. Biomol. Screen 2008 10.1177/1087057108319644.

(4). Gordon AJ; Ford RA The Chemist's Companion: A Handbook of Practical Data, Techniques, and References, 1 edition; Wiley: New York, 1972.

(5). Attimarad M; Ahmed KKM; Aldhubaib BE; Harsha S High-Performance Thin Layer Chromatography: A Powerful Analytical Technique in Pharmaceutical Drug Discovery. Pharm. Methods 2011, 2 (2), 71–75. 10.4103/2229-4708.84436. [PubMed: 23781433]

(6). Fichou D; Morlock GE Open-Source-Based 3D Printing of Thin Silica Gel Layers in Planar Chromatography. Anal. Chem 2017, 89 (3), 2116–2122. 10.1021/acs.analchem.6b04813. [PubMed: 28208299]

(7). Morlock GE; Oellig C; Bezuidenhout LW; Brett MJ; Schwack W Miniaturized Planar Chromatography Using Office Peripherals. Anal. Chem 2010, 82 (7), 2940–2946. 10.1021/ac902945t. [PubMed: 20155949]

(8). Stroka J; Spangenberg B; Anklam E New Approaches in Tlc-Densitometry. J. Liq. Chromatogr. Relat. Technol 2002, 25 (10–11), 1497–1513. 10.1081/JLC-120005700.

(9). Lancaster M; Goodall DM; Bergström ET; McCrossen S; Myers P Real-Time Image Acquisition for Absorbance Detection and Quantification in Thin-Layer Chromatography. Anal. Chem 2006, 78 (3), 905–911. 10.1021/ac051390g. [PubMed: 16448067]

(10). Morlock G; Schwack W Planar Chromatography Coupled to Mass Spectrometry. TrAC Trends Anal. Chem 2010, 29, 1157–1171. 10.1016/j.trac.2010.07.010.

(11). Ferenczi-Fodor K; Végh Z; Renger B Thin-Layer Chromatography in Testing the Purity of Pharmaceuticals. TrAC Trends Anal. Chem 2006, 25, 778–789. 10.1016/j.trac.2006.06.003.

(12). Jo HH; Gao X; You L; Anslyn EV; Krische MJ Application of a High-Throughput Enantiomeric Excess Optical Assay Involving a Dynamic Covalent Assembly: Parallel Asymmetric Allylation and Ee Sensing of Homoallylic Alcohols. Chem. Sci 2015, 6 (12), 6747–6753. 10.1039/C5SC02416A. [PubMed: 27014433]

(13). Diehl KL; Kolesnichenko IV; Robotham SA; Bachman JL; Zhong Y; Brodbelt JS; Anslyn EV Click and Chemically Triggered Declick Reactions through Reversible Amine and Thiol Coupling via a Conjugate Acceptor. Nat. Chem 2016, 8 (10), 968–973. 10.1038/nchem.2601.

(14). Poole CF; Poole SK Instrumental Thin-Layer Chromatography. Anal. Chem 1994, 66 (1), 27A–37A. 10.1021/ac00073a001.

(15). Thoden J Spotter for Use in Thin Layer Chromatography and Method of Forming Drops Therewith. US3843053A, 10 22, 1974.

(16). Musil F; Fosslien E An Automatic Eight-Channel Spot Applicator for Thin-Layer Chromatography. J. Chromatogr. A 1970, 47, 116–118. 10.1016/0021-9673(70)80017-6.

(17). Terol-Villalobos IR; Mendiola-Santibañez JD Transformations with Reconstruction Criteria: Image Segmentation and Filtering In Mathematical Morphology: 40 Years On;Ronse C, Najman L, Decencière E, Eds.; Computational Imaging and Vision; Springer Netherlands: Dordrecht, 2005; pp 75–84. 10.1007/1-4020-3443-1_8.

(18). Meyer KH Fritz Ullmann 1875–1939. Helv. Chim. Acta 1940, 23 (1), 93–100. 10.1002/hlca.19400230110.

(19). van der Walt S; Schönberger JL; Nunez-Iglesias J; Boulogne F; Warner JD; Yager N; Gouillart E; Yu T Scikit-Image: Image Processing in Python. PeerJ 2014, 2, e453 10.7717/peerj.453. [PubMed: 25024921]

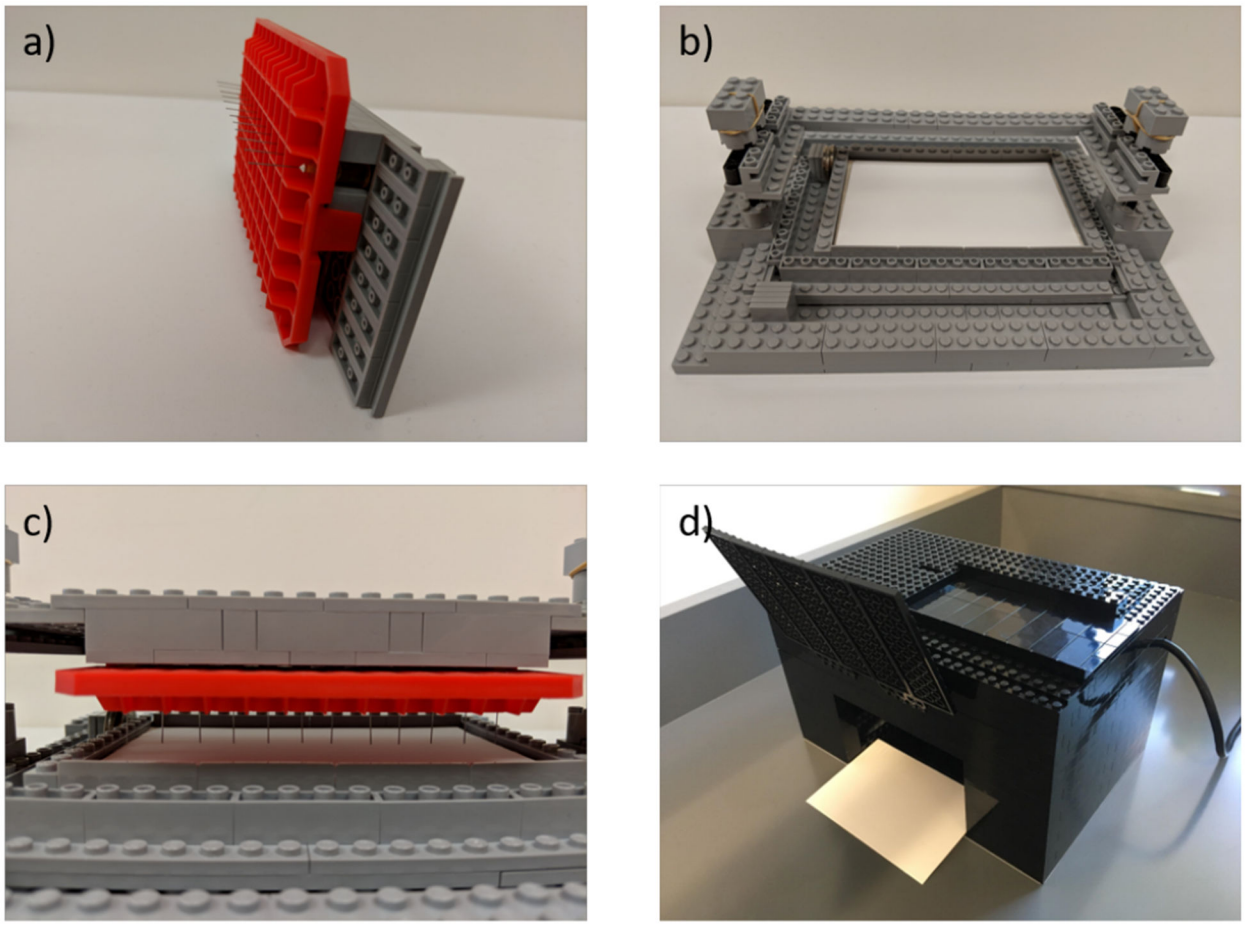

Figure 1.

a) The LEGO™ holder to be loaded with blunted syringe needles, b) TLC carriage, c) LEGO™ spotter/holder placed on carriage. d) LEGO™ black-box with UV-lamp in back.

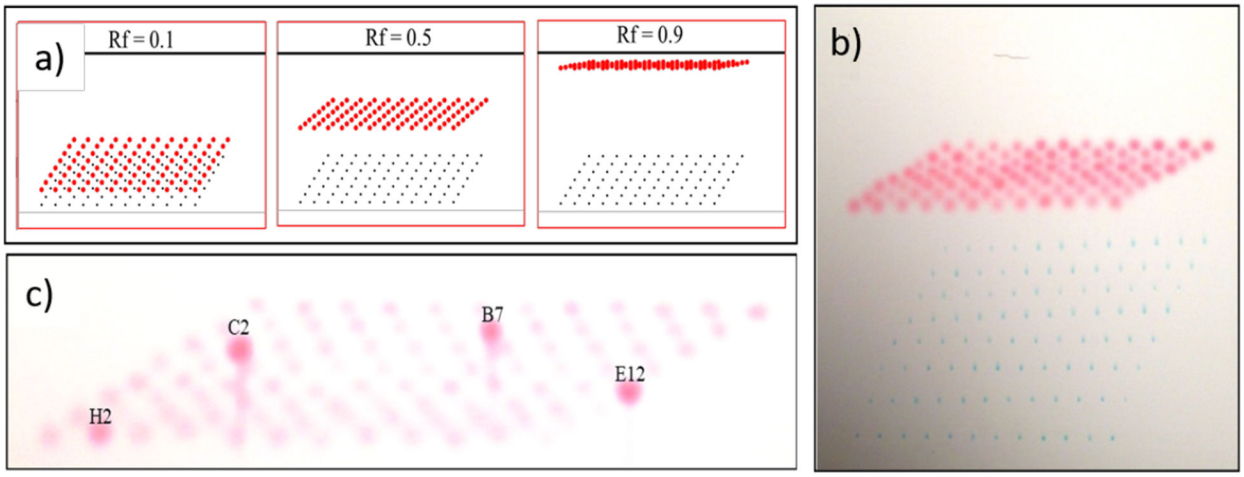

Figure 2.

Modeling and initial studies using dyes from multi-parallel from microplates spotted on TLC plates using a staggered spotting approach. a) Excel modeling showing 'sweet spot' of R_f ~0.5 for most effective visualization. b) Elution of spots from a 96-well plate containing samples of methylene blue (R_f ~0) and methyl red (R_f ~0.6) using 95% ethanol/water. c) Analysis of plate, not eluted, containing 4 wells spiked with additional methyl red allows easy determination of the 'address' of the hits.

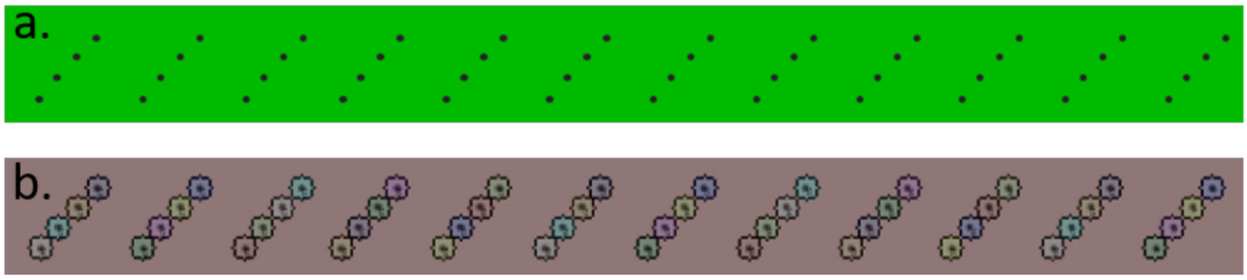

Figure 3.
a) A computer-generated model TLC plate. b) The model TLC plate post software analysis.

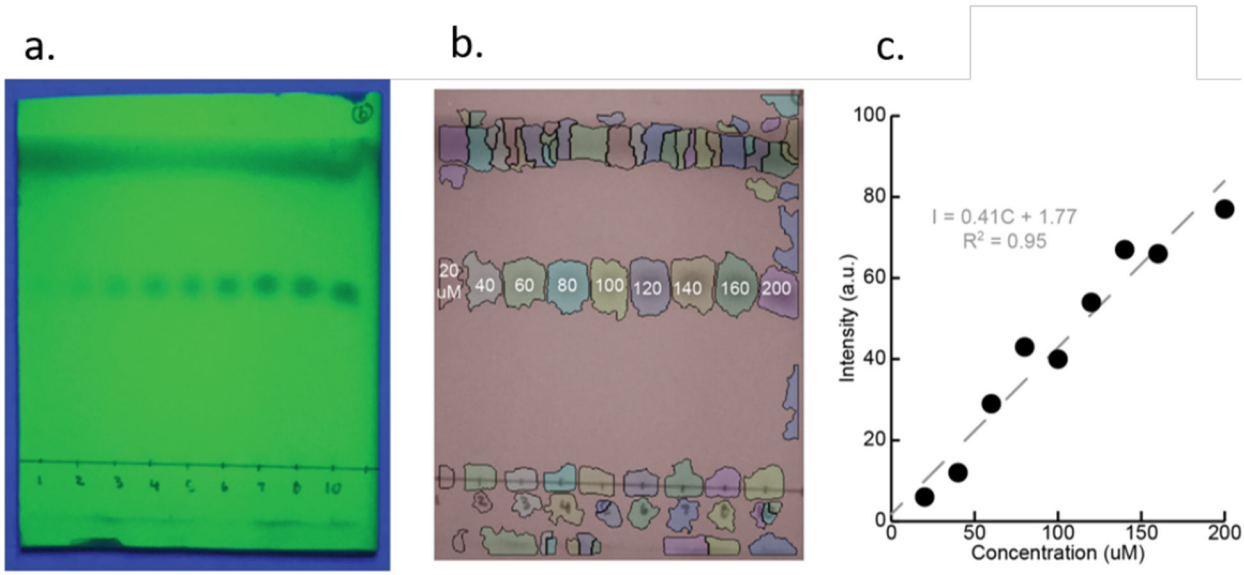

Figure 4.

a) A calibration plate is spotted with known concentrations of analyte **1** and eluted. b) Eluted spots are segmented and their intensities are quantified. Loading concentration of each reaction is indicated in μM. c) A linear calibration curve (R^2 = 0.95) generated from varying concentration of **1**.

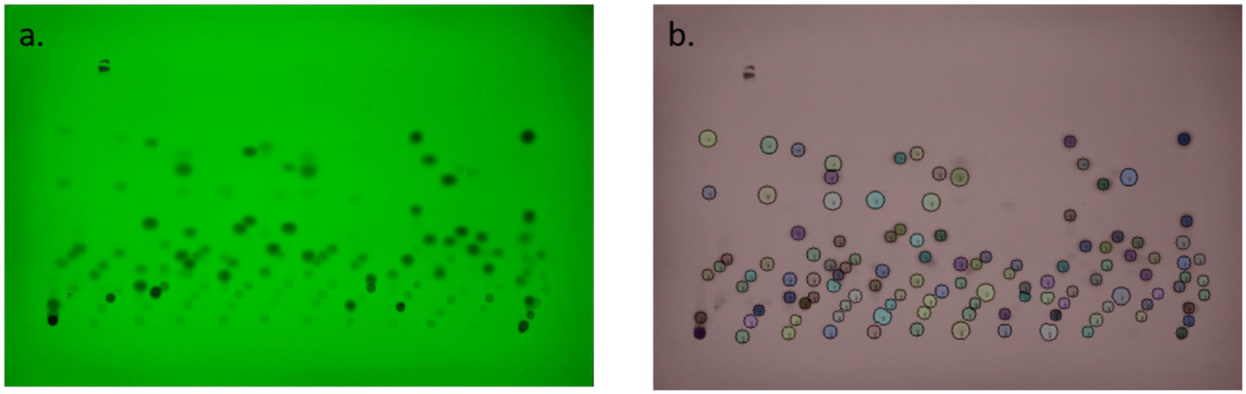

Figure 5.
(a) An eluted TLC plate spotted with 48 reactions. (b) A sci-kit analyzed image of the eluted TLC plate.

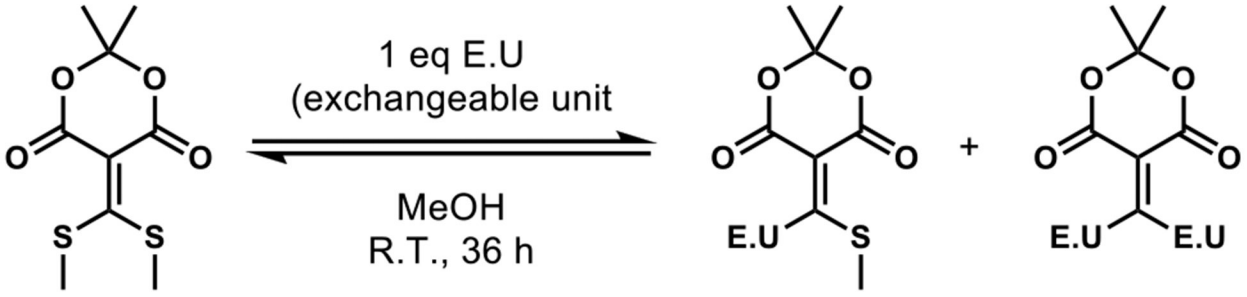

Scheme 1.

Meldrum's acid derived conjugate acceptor **1** with various thiols or amines as nucleophiles. E.U. = Exchangeable Unit.

Table 1.

Percent composition of **1** obtained using NMR and LCMS spectrum. All yields were determined via NMR except when marked by an "*" to denote the yield was determined via LC/MS.

	TLC Spot Intensity	TLC Yield	Assay Yield	Error
Control	70	-	-	-
1,4-phenylenediamine	0	100	100	0
1-dodecanethiol	55	21	12	9
2-mercaptoethanol	72	−3	0	2
1,4-butanedithiol	86	−23	10	33
3,6-dioxa-1,8-octane-dithiol	57	19	0	22
p-Xylylenediamine	0	100	100	0
1-decanethiol	67	4	20	16
4-methoxybenzylamine	0	100	96	4
dodecylamine	0	100	100	0
N-benzylmethylamine	0	100	94*	6
			AVG. ERROR	9